Supplementary Information

Penta-MS_2 (M = Mn, Ni, Cu/Ag and Zn/Cd) Monolayers with Negative Poisson's Ratios and Tunable Bandgaps as Water-Splitting Photocatalysts

Xiaodong Lv,[1] Linke Yu,[1] Fengyu Li,[1,*] Jian Gong,[1,*] Yong He,[2] Zhongfang Chen[3,*]

[1] *School of Physical Science and Technology, Inner Mongolia University, Hohhot, 010021, China*

[2] *State Key Laboratory for Artificial Microstructures and Mesoscopic Physics, School of Physics, Peking University, Beijing, 100871, China*

[3] *Departm ent of Chemistry, The Institute for Functional Nanomaterials, University of Puerto Rico, Rio Piedras Campus, San Juan, PR 00931, USA*

*corresponding authors: fengyuli@imu.edu.cn (FL); ndgong@imu.edu.cn (JG); zhongfangchen@gmail.com (ZC)

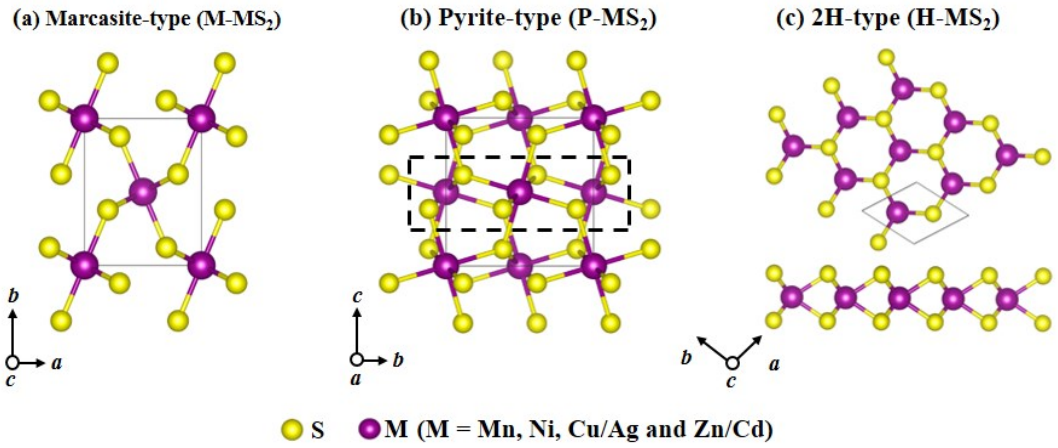

Fig. S1 The MS_2 (M = Mn, Ni, Cu/Ag and Zn/Cd) structures of (a) bulk marcasite phase and (b) bulk pyrite phase. (c) The top and side views of hexagonal H-MS_2 monolayer. Dashed box represent an isolated monolayer of pyrite phase.

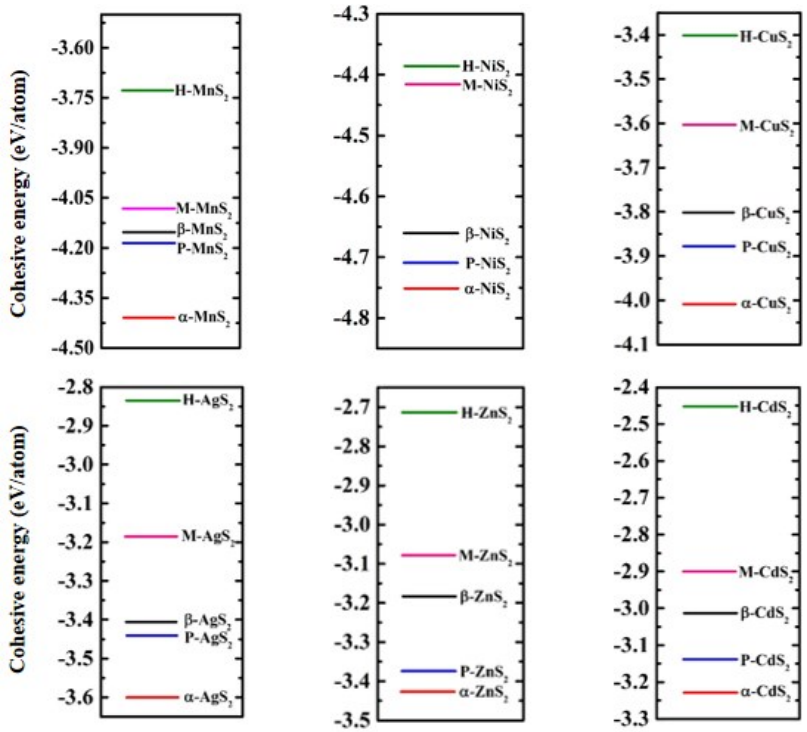

Fig. S2 The cohesive energy of pentagonal MS_2 (M = Mn, Ni, Cu/Ag and Zn/Cd) monolayer in α-, β, P, M and H-type structures.

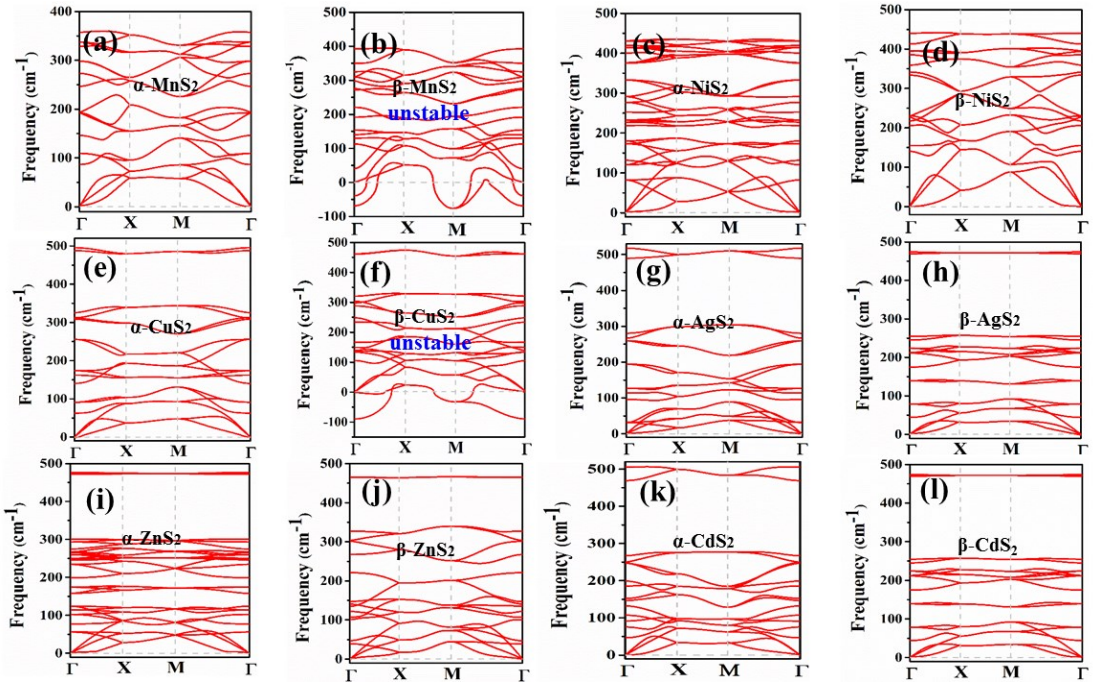

Fig. S3 The calculated phonon spectra of the pentagonal α-MS_2 and β-MS_2 (M = Mn, Ni, Cu/Ag and Zn/Cd) monolayers.

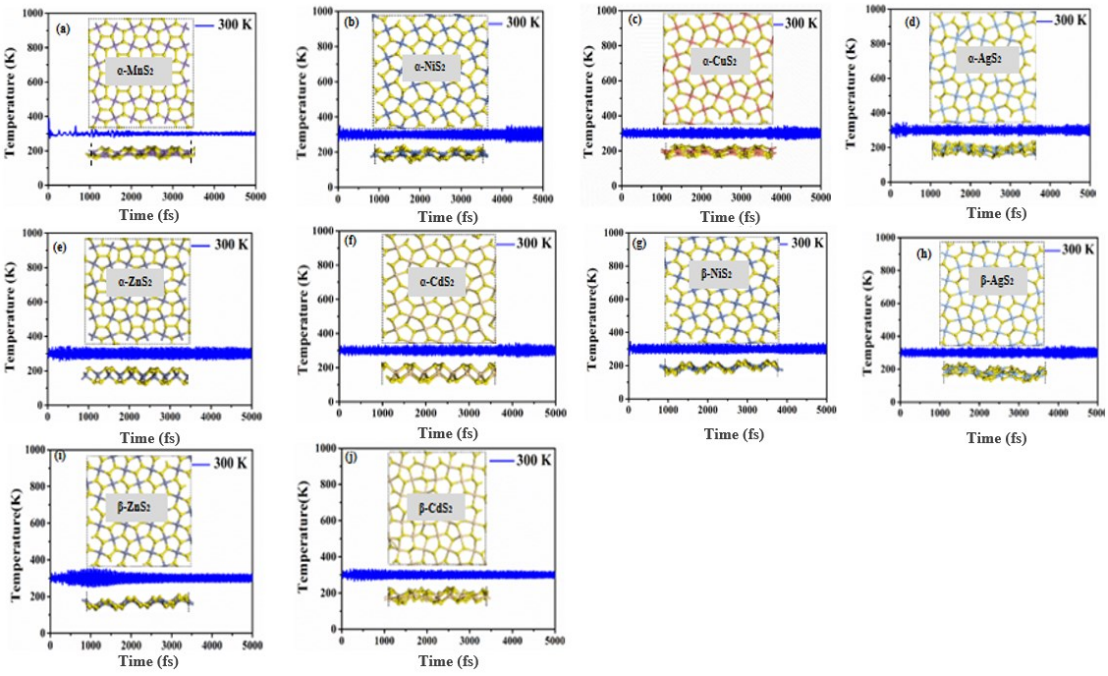

Fig. S4 Time evolution of temperature during the first-principles molecular dynamics (FPMD) simulations of (a-f) α-MS_2 (M = Mn, Ni, Cu/Ag and Zn/Cd) and (g-j) β-MS_2 (M = Ni, Ag, Zn and Cd) monolayers with a 4 × 4 × 1 supercell at 300 K for 5 ps. The insets are the snapshots taken from the end of the FPMD simulations.

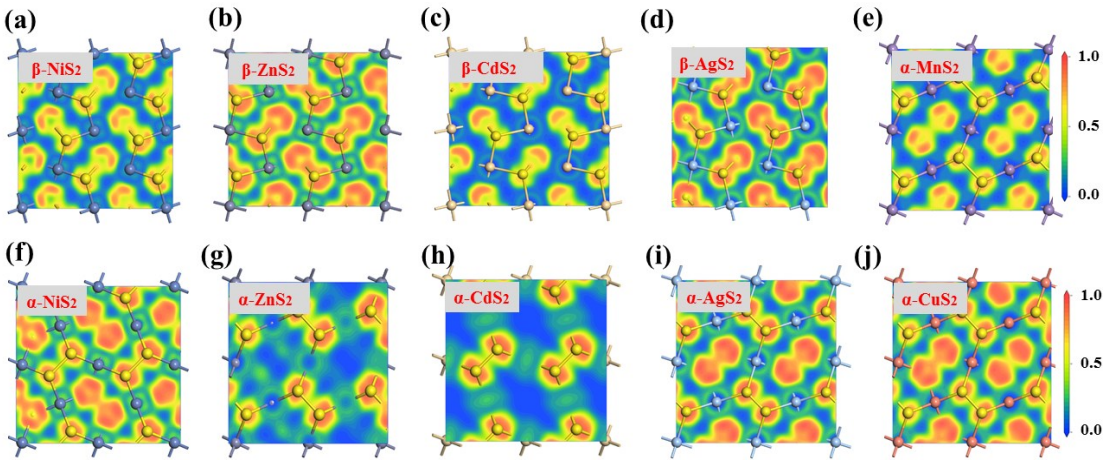

Fig. S5 The electronic localization function (ELF) for β-MS_2 (a-d) and α-MS_2 (e-j) monolayers. In the ELF maps, the red and blue colors refer to the highest value (1.00) and the lowest value (0.00) of ELF, respectively. Corresponding to the accumulation and depletion of electrons in the two colored regions.

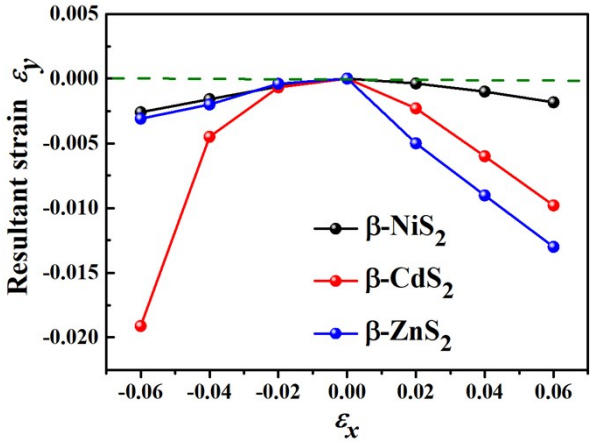

Fig. S6 The response of *y*-axial lattice to the uniaxial stains along *x*-direction for β-MS_2 (M = Ni, Zn and Cd) monolayers.

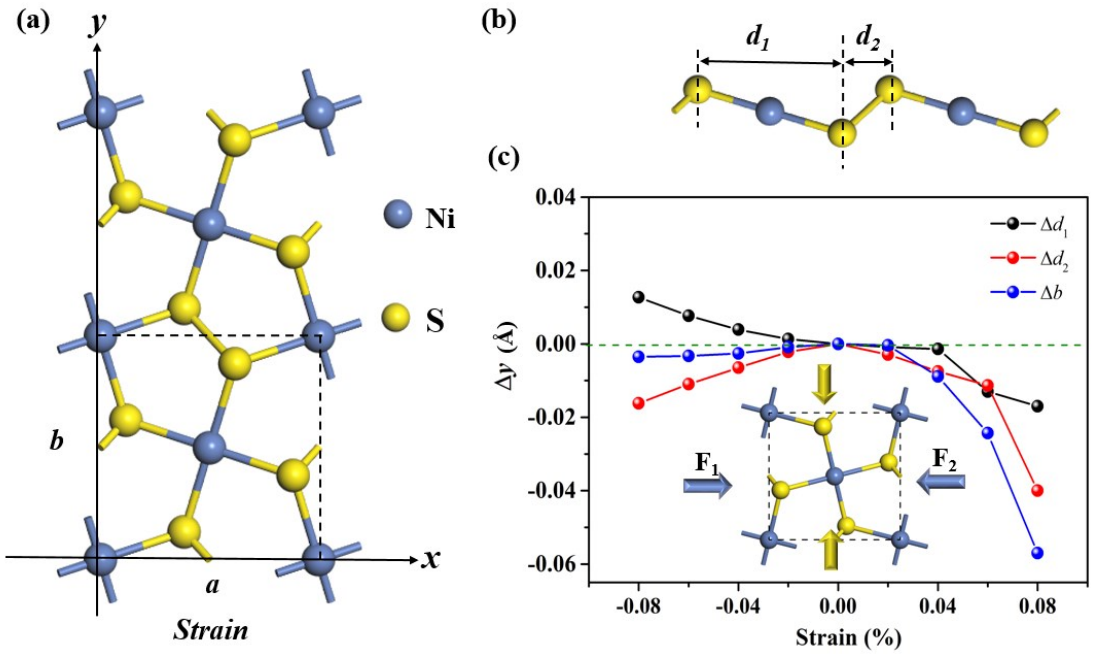

Fig. S7 (a) The top view of β-NiS_2 monolayer and (b) the side view along *y* direction, (c) the black (Δd_1), red (Δd_2) and blue ($\Delta b=\Delta d_1+\Delta d_2$) lines represent the variations of *y*-projections of S−Ni−S and S−S lengths, and the change of lattice *b*, respectively.

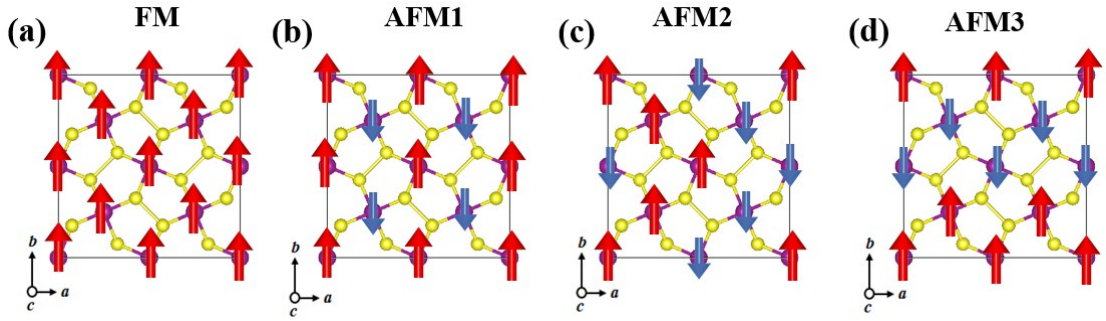

Fig. S8 The four different magnetic configurations of pentagonal α-MnS_2 monolayer: (a) FM, (b) AFM1, (c) AFM2 and (d) AFM3.

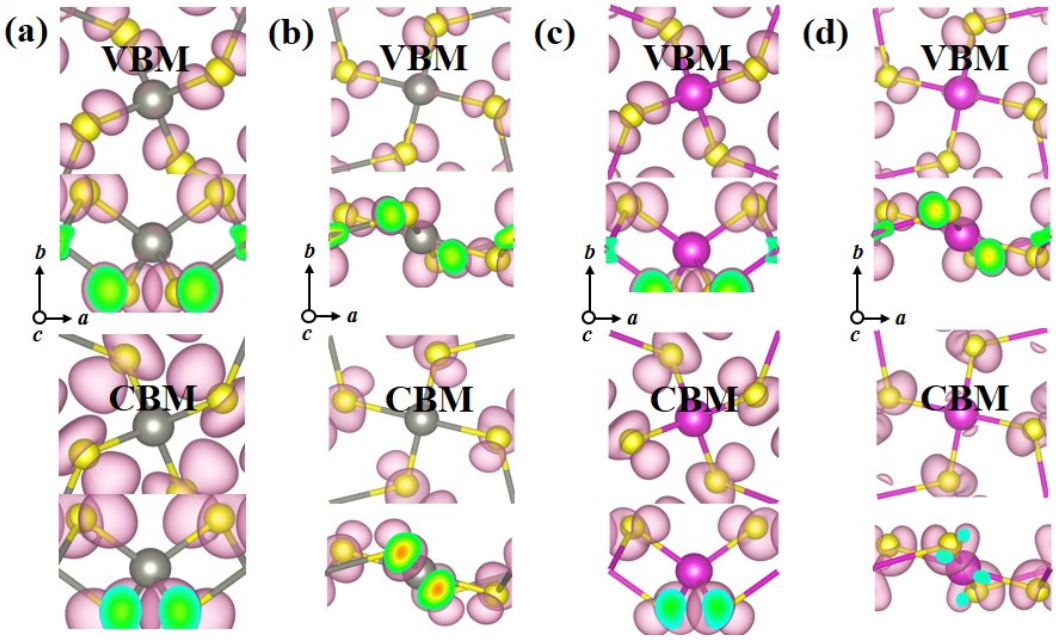

Fig. S9 The spatial charge density of VBM and CBM of pentagonal (a) α-ZnS_2, (b) β-ZnS_2, (c) α-CdS_2 and (d) β-CdS_2 monolayer, respectively. The charge density isosurfaces are set with 0.004 e Å^{-3}.

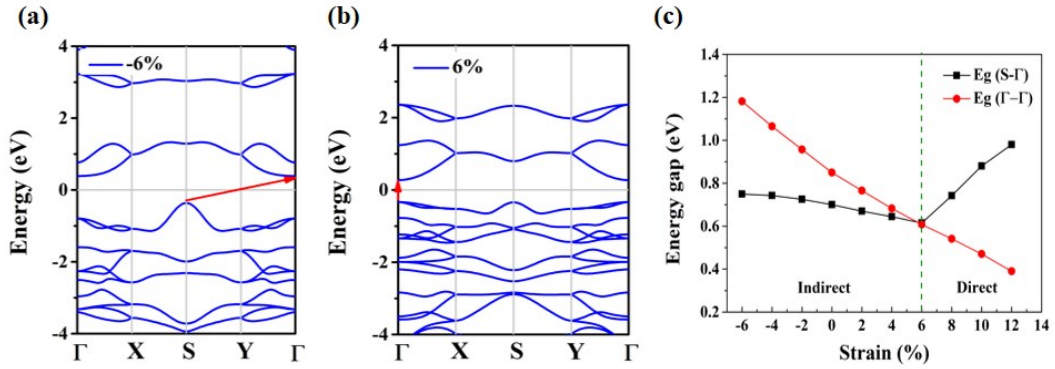

Fig. S10 Strain-induced electronic band structure for α-NiS_2 monolayer. (a, b) Band structure under a compression and tensile strain of 6%, respectively; (c) the energy gaps versus biaxial strains. The E_g (S_Γ) denotes the gap between the highest occupied band at the S point and the lowest unoccupied band at the Γ point, the E_g (Γ_Γ) represents the gap between the highest occupied band and the lowest unoccupied band both at the Γ point.

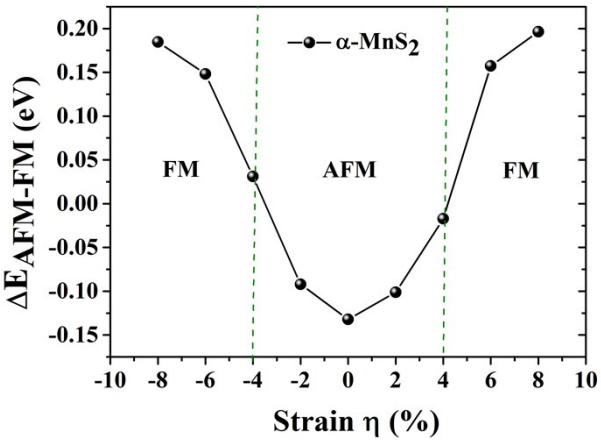

Fig. S11 The energy difference between AFM and FM states ($\Delta E_{\text{AFM-FM}}$) of the pentagonal α-MnS_2 monolayer as a function of biaxial strain η. A negative (positive) $\Delta E_{\text{AFM-FM}}$ value indicates that AFM (FM) is the ground state.

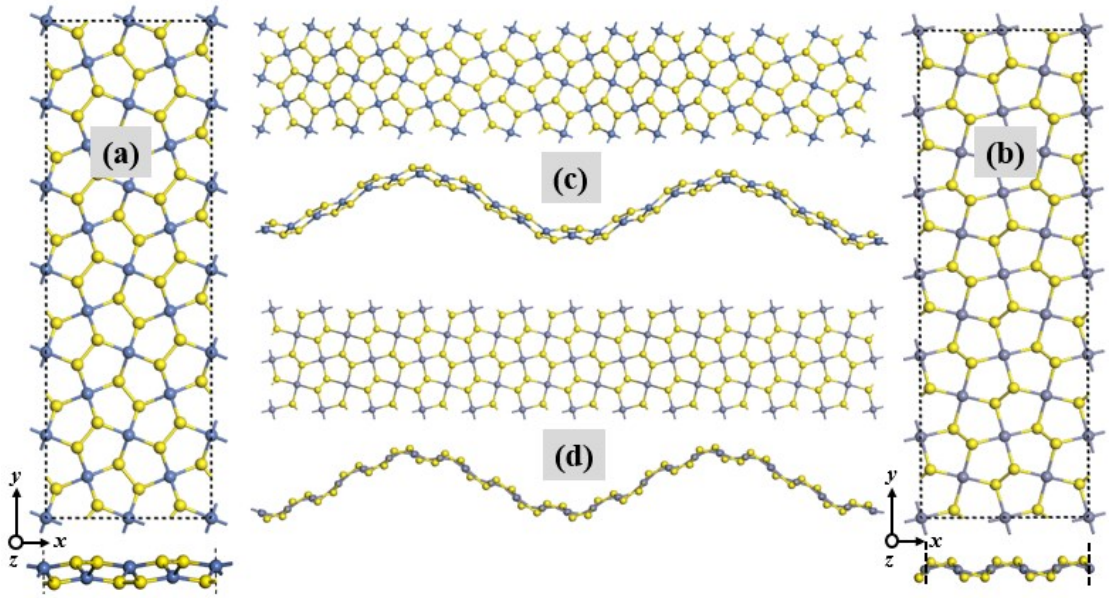

Fig. S12 The structures of (a) α-NiS_2 and (b) β-ZnS_2 monolayers without compression. The top and side views of (c) waved pentagonal α-NiS_2 and (d) waved pentagonal β-ZnS_2 monolayers along *y* direction.

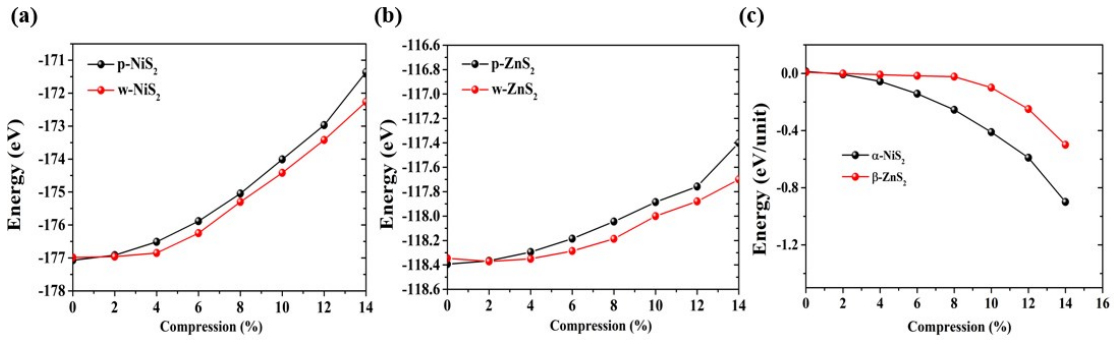

Fig. S13 (a, b) The energies of uncambered 2D monolayer (u-MS_2) and waved (w-MS_2) as a function of *y*-axial compression. (c) Energy difference between uncambered and waved of pentagonal MS_2 under the same compression as calculated from E_{dif} = (E(w-MS_2)-E(u-MS_2))/N [*ACS Appl. Nano Mater.* 2020, 3, 2804], where N is the number of unit cell in a supercell. N was adopted 6 in our test computations.

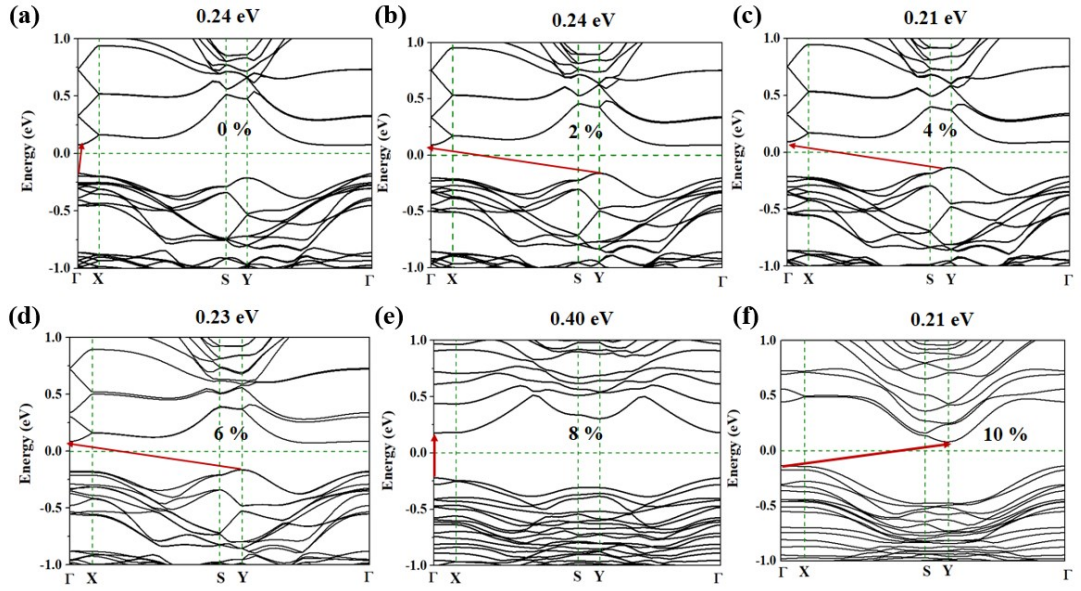

Fig. S14 The PBE band structure of waved α-NiS_2 under uniaxial compressions of (a) 0%, (b) 2%, (c) 4%, (d) 6%, (e) 8% and (f) 10%.

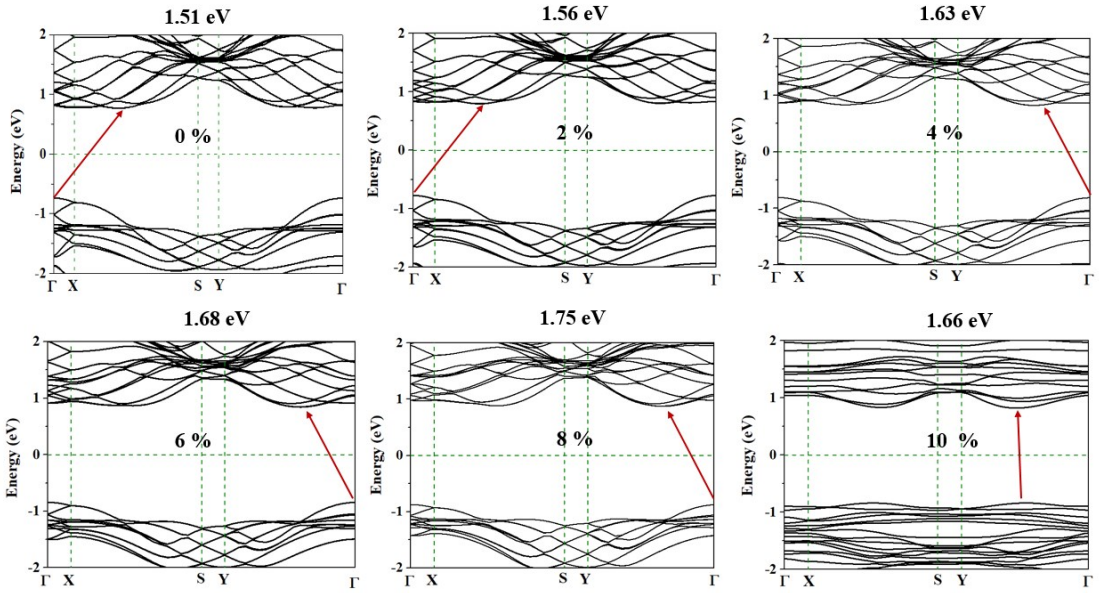

Fig. S15 The PBE band structure of waved β-ZnS_2 under uniaxial compressions of (a) 0%, (b) 2%, (c) 4%, (d) 6%, (e) 8% and (f) 10%.

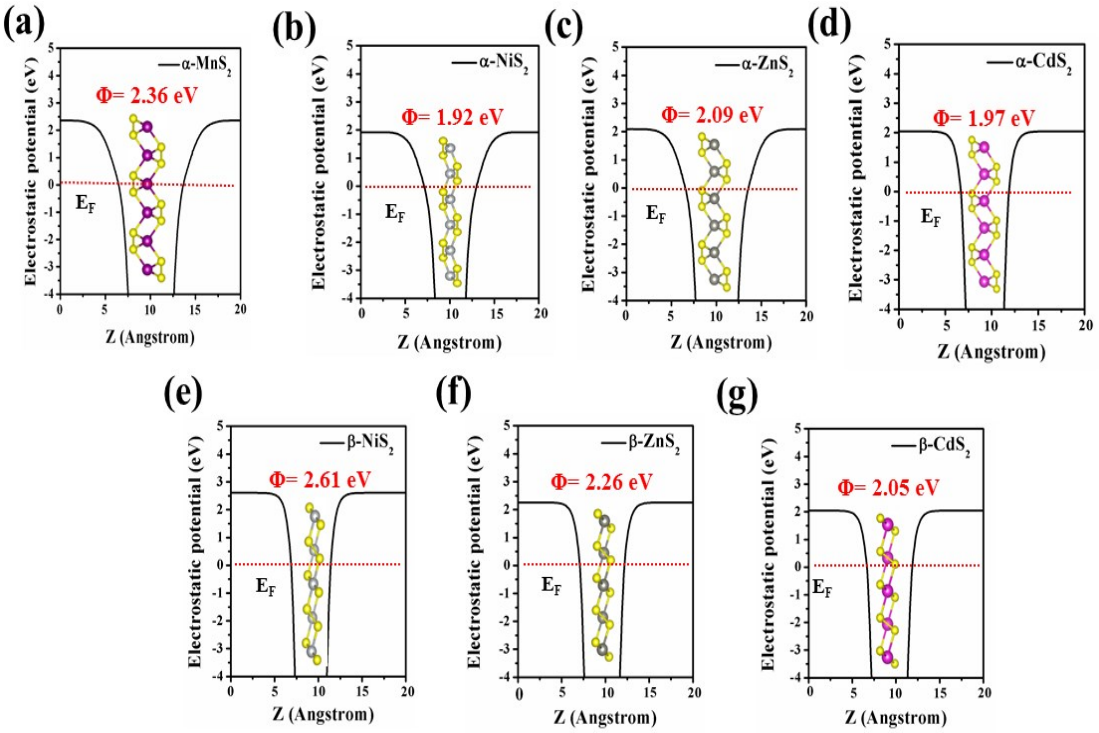

Fig. S16 The calculated electrostatic potential in a vacuum region for (a-d) α-MS_2 (M = Mn, Ni, Zn and Cd) and (e-g) β-MS_2 (M = Ni, Zn and Cd) monolayers based on HSE06 method.

Table S1. The lattice constants (*a* and *b*, in Å), M−S bond length ($d_{M–S}$, in Å), S−S bond length ($d_{S–S}$, in Å), thickness (*h*, Å) and cohesive energy (E_{coh}, in eV/atom) of penta-MS_2 monolayers, marcasite/pyrite-type bulk and 2H-type MS_2 (M = Mn, Ni, Cu/Ag and Zn/Cd) monolayer structures (noted as α-MnS_2, β-MnS_2, M-MS_2, P-MS_2 and 2H-MS_2, respectively). The most negative E_{coh} values were highlighted in bold.

System	*a*	*b*	$d_{M–S}$	$d_{S–S}$	*h*	E_{coh}
α-MnS_2	5.67	5.67	2.20	2.21	0.20	**-4.37**
β-MnS_2	5.66	5.70	2.24	2.22	0.62	-4.14
M-MnS_2	4.51	5.22	2.45	--	--	-4.13
P-MnS_2	5.50	5.50	2.31	2.09	--	-4.17
H-MnS_2	3.08	3.08	2.28	3.08	--	-3.69
α-NiS_2	5.28	5.28	2.14	2.13	1.36	**-4.75**
β-NiS_2	5.21	5.32	2.17	2.13	1.15	-4.66
M-NiS_2	4.60	5.18	2.16	--	--	-4.01
P-NiS_2	5.59	5.59	2.36	2.03	--	-4.71
H-NiS_2	3.53	3.53	2.29	3.52	--	-4.39
α-CuS_2	5.50	5.50	2.26	2.10	1.41	**-4.01**
β-CuS_2	5.56	5.67	2.32	2.07	1.38	-3.80
M-CuS_2	4.91	5.09	2.15	--	--	-3.60
P-CuS_2	5.79	5.79	2.46	2.02	--	-3.87
H-CuS_2	3.12	3.12	2.36	3.12	--	-3.40
α-AgS_2	6.00	6.00	2.48	2.02	1.35	**-3.60**
β-AgS_2	5.95	6.06	2.51	2.03	1.12	-3.42
M-AgS_2	5.27	5.32	2.39	--	--	-3.19
P-AgS_2	6.23	6.23	2.67	2.00	--	-3.43
H-AgS_2	3.31	3.31	2.56	3.32	--	-2.82
α-ZnS_2	5.06	5.06	2.35	2.10	2.67	**-3.41**
β-ZnS_2	5.83	5.48	2.53	2.10	1.40	-3.17
M-ZnS_2	4.84	5.11	2.22	--	--	-3.08
P-ZnS_2	6.00	6.00	2.54	2.08	--	-3.39
H-ZnS_2	3.23	3.23	2.47	3.23	--	-2.71
α-CdS_2	5.46	5.46	2.58	2.10	2.95	**-3.23**
β-CdS_2	6.01	5.96	1.55	2.68	1.55	-3.01
M-CdS_2	4.93	5.52	2.44	--	--	-2.90
P-CdS_2	6.42	6.42	2.74	2.08	--	-3.14
H-CdS_2	3.33	3.33	2.68	3.33	--	-2.45

Table S2. The calculated energies of the ferromagnetic (E_{FM}) and antiferromagnetic states (E_{AFM}), as well as the corresponding exchange energy (E_{ex}) and the magnetic moments (M_{total}). The exchange energy is defined as $E_{ex} = (E_{FM} - E_{AFM})$ for a 2×2×1 supercell.

α-MnS_2	E_{total} (eV)	E_{ex} (meV)	M_{total} (μ_B)
FM	-144.678	0	23.99
AFM1	-145.214	536	0
AFM2	-144.720	42	0
AFM3	-145.130	452	0

Table S3. Energy difference (meV/unit cell) among anti-ferromagnetic (AFM), ferromagnetic (FM), and non-magnetic (NM) states in pentagonal unit cell of α-MS_2 (M = Mn, Ni, Cu/Ag and Zn/Cd) and β-MS_2 (M = Ni, Ag, Zn and Cd) monolayers with and without strain (η = -8%~8%). The AFM state refers to the lowest-energy AFM1.

	E_{AFM}-E_{FM}									E_{AFM}-E_{NM}								
η	-8	-6	-4	-2	0	2	4	6	8	-8	-6	-4	-2	0	2	4	6	8
α-MnS_2	184	148	-31	-92	-135	-101	-17	157	196	-85	-160	-290	-490	-540	-490	-304	-50	-24
α-NiS_2	0	0	0	0	0	0	0	0	0	0	0	0	0	5	0	0	0	0
α-CuS_2	0	0	0	0	1	0	0	0	0	0	0	0	0	4	0	0	0	0
α-AgS_2	0	0	0	0	2	0	0	0	0	0	0	0	0	3	0	0	0	0
α-ZnS_2	0	0	0	0	0	0	0	0	0	0	0	0	0	6	0	0	0	0
α-CdS_2	0	0	0	0	0	0	0	0	0	0	0	0	0	0	0	0	0	0
β-NiS_2	0	0	0	0	0	0	3	0	0	27	45	60	72	100	84	65	33	16
β-AgS_2	0	0	0	0	0	0	0	0	0	0	0	0	0	1	0	0	0	0
β-ZnS_2	0	0	2	0	0	0	0	0	0	0	0	0	0	0	0	1	0	0
β-CdS_2	0	1	0	0	0	0	0	0	0	0	0	0	0	0	0	0	0	0

Table S4. Bader charge and Hirshfeld charge analysis of pentagonal α-MS_2 (M = Mn, Ni, Cu/Ag and Zn/Cd) and β-MS_2 (M = Ni, Ag and Zn/Cd) monolayers.

Charge	Bader-M	Bader-S_2	Hirshfeld-M	Hirshfeld-S_2
α-MnS_2	+0.96	-0.96	+0.29	-0.29
α-NiS_2	+0.23	-0.23	+0.05	-0.05
β-NiS_2	+0.24	-0.24	+0.06	-0.06
α-CuS_2	+0.45	-0.45	+0.14	-0.14
α-AgS_2	+0.22	-0.22	+0.16	-0.16
β-AgS_2	+0.45	-0.45	+0.17	-0.17
α-ZnS_2	+0.48	-0.48	+0.20	-0.20
β-ZnS_2	+0.84	-0.84	+0.29	-0.29
α-CdS_2	+0.75	-0.75	+0.26	-0.26
β-CdS_2	+0.89	-0.89	+0.35	-0.35

Table S5. The in-plane Poisson's ratios of pentagonal β-MS_2 (M = Ni, Zn, and Cd) monolayer and other reported 2D sheets.

Structures	ν_x (ν_y)
Penta-graphene	-0.068[a]
Phosphorene	-0.027[b]
Borophene	-0.022(-0.002)[c]
β-NiS_2 (this work)	-0.010(-0.020)
β-ZnS_2 (this work)	-0.50
β-CdS_2 (this work)	-0.39

[a] S. Zhang, J. Zhou, Q. Wang, X. Chen, Y. Kawazoe and P. Jena, Penta-graphene: a new carbon allotrope, *Proc. Nat. Acad. Sci*., 2015, **112**, 2372–2377.

[b] J. Jiang and H. Park, Negative poisson's ratio in single-layer black phosphorus, *Nat. Commun*., 2014, **5**, 4727.

[c] H. Zhong, K. Huang, G. Yu, and S. Yuan, Electronic and mechanical properties of few-layer borophene, *Phys. Rev. B*., 2018, **98**, 054104.